Table 1 History of HAM/TSP patients and effect of PPS treatment on lower-extremity motor function and spasticity

	1	2	3	4	5	6	7	8	9	10	11	12
Age (years)	57	62	61	49	64	76	63	67	77	62	73	63
Sex	Male	Female	Female	Female	Male	Male	Female	Female	Female	Female	Female	Female
Duration of illness (years)	51	28	30	29	11	23	15	3	17	12	52	19
Concomitant therapy	PSL/IFN-α	No	No	No	PSL	No	No	No	No	PSL	No	No
OMDS[a]												
Before treatment	6	10	5	5	5	6	4	3	5	4	10	4
After treatment[b]	5	10	5	5	5	6	4	3	5	4	10	4
Spasticity of lower extremities												
Before treatment	Yes	Yes	Yes	Yes	Yes	Yes	Yes	No	Yes	No	No	Yes
Improvement[c]												
None		○										
One grade			○	○	○	○	○		○			
Two grades	○											○

PSL prednisolone, *IFN-α* interferon-alpha

○ indicates the status of the improvement of spasticity

[a] OMDS score was 0–13 according to disability grade (Osame et al. 1989)

[b] Evaluated at 1 week after final injection

[c] Improvement in spasticity of more than one grade according to the Modified Ashworth Scale (Bohannon and Smith 1987) was evaluated at 1 week after final injection

PPS treatment

PPS (pentosan polysulfate SP 54; bene-Arzneimittel GmbH, Munich, Germany) was administered subcutaneously once weekly. A dose of 25 mg was administered in treatment week 1 (commencement), 50 mg in week 2, and 100 mg in weeks 3–8. This PPS dosage schedule was the same as that used in a previous clinical trial for patients with knee osteoarthritis (Kumagai et al. 2010). We monitored activated clotting time (ACT), APTT, and PT international normalized ratio (PT-INR) 1 h after the administration of PPS.

Assessment of effects of PPS treatment

Neurological assessment

Each week, we monitored changes in motor function score using Osame's Motor Disability Scale (OMDS) (Osame et al. 1989). Spasticity of the lower extremities was also graded each week with the Modified Ashworth Scale (Bohannon and Smith 1987). We also calculated the percentage reduction in the time required to walk 10 m or down a flight of stairs, as follows: (time required at commencement of PPS treatment − time required/time required at commencement of PPS treatment) × 100. The clinical investigators were blinded to the laboratory investigations and assessments such as HTLV-I proviral load, soluble adhesion molecules, and chemokines.

HTLV-I proviral load in peripheral blood mononuclear cells

We monitored the changes in HTLV-I proviral load in peripheral blood mononuclear cells (PBMCs) at the commencement of PPS treatment (treatment week 1), treatment week 3, and at 1 and 5 weeks after the final injection. For quantitative analysis of HTLV-I proviral load, real-time quantitative PCR was performed in a LightCycler FastStart DNA Master (Roche Diagnostics, Mannheim, Germany) based on general fluorescence detection with SYBR Green, as described previously (Nishiura et al. 2009). Genomic DNA samples from PBMCs from HAM/TSP patients were prepared using a Genomic DNA Extraction kit (Wako Pure Chemical Industries Ltd., Osaka, Japan). DNA samples were subjected to real-time PCR in a LightCycler PCR system using Tax-specific primers, forward primer (5′-AAACAGCCCTGCAGATACAAAGT-3′), and reverse primer (5′-ACTGTAGAGCTGAGCCGA TAACG-3′), and β-actin-specific primers, forward primer (5′-GCCCTCATTTCCCTCTCA-3′) and reverse primer (5′-GCTCAGGCAGGAAAGACAC-3′). The PCR conditions for the Tax-specific primers were 40 cycles of denaturation (95 °C, 15 s), annealing (55 °C, 5 s), and extension (72 °C, 10 s), and those for the β-actin primers were 32 cycles of denaturation (95 °C, 15 s), annealing (62 °C, 5 s), and extension (72 °C, 15 s). The HTLV-I proviral load per 10,000 cells was calculated according to the following formula: (copy number of Tax/copy number of β-actin/2) × 10,000.

Measurement of soluble adhesion molecules and chemokines in serum

The concentration of soluble vascular cell adhesion molecule VCAM (sVCAM)-1, soluble intercellular adhesion molecule (sICAM)-1, chemokine CXC ligand (CXCL)10, and chemokine CC ligand (CCL)2 in serum was measured using an ELISA kit (MILLIPLEX® MAP kit, Millipore Corporation, Billerica, MA, USA) on MAGPIX with xPONENT software (Merck Millipore Co., USA) in accordance with the manufacturer's instructions. All samples were analyzed 20-fold diluted for sVCAM-1 and sICAM-1 and 4-fold diluted for CXCL10 and CCL2 in duplicate and on the same plate. The detection ranges for these assays were 61–250,000 pg/ml for sVCAM-1 and sICAM-1 and 3.2–10,000 pg/ml for CXCL10 and CCL2, respectively. We calculated the percentage increase for serum sVCAM-1 level as follows: (serum level of sVCAM-1at 1 week after final injection−level at commencement of PPS treatment/level at commencement of PPS treatment)×100.

Co-cultivation

We used HCT-5 which is an HTLV-I-infected T cell line derived from the cerebrospinal fluid of an HAM/TSP patient (Fukushima et al. 2008) and H9/K30 *luc* reporter cells which are lymphocytic H9 cells stably transfected with a plasmid containing the gene encoding luciferase under the control of the HTLV-I long terminal repeat (LTR) (Yoshida et al. 2005) (kindly provided by Prof. Akio Adachi, University of Tokushima Graduate School, Japan). HCT-5 (5×10^5 cells) were co-cultivated in the presence of various concentrations of PPS with H9/K30 *luc* reporter cells (3.5×10^5 cells) in 24-well culture plate at 37 °C under 5 % CO_2. After co-cultivation for 24 h, luciferase activity was assessed by using a luciferase assay system (Promega, Madison, USA) and Luminometer TD-20/20 (Turner Designs Instrument, USA). The relative luc activity was calculated according to the following formula: relative luminescent units (RLU) of co-cultivated sample/RLU of the H9-only-cultivated sample. Data were expressed as mean±SD of triplicate cultures.

Statistical analysis

Data were analyzed using Student's *t* tests and the Wilcoxon signed-rank test. Data for the reduction in time required to walk 10 m or down a flight of stairs were analyzed using the Wilcoxon signed-rank test or the Kruskal–Wallis test. If significance was detected, Steel's test for post hoc comparison was performed to compare the effect of treatment with the data at the commencement of treatment. Correlation analysis was performed by use of nonparametric Spearman's rank correlation test. Differences were considered statistically significant for $p<0.05$.

Results

Clinical effects

Improvement of spasticity

Improvement of motor disability score was observed only in patient 1 when evaluated at 1 week after the final injection (Table 1). However, according to evaluation with the Modified Ashworth Scale, among the nine patients in whom lower extremity spasticity was observed before treatment, six showed improvement of one grade following treatment, and two patients demonstrated an improvement of two grades, when evaluated at 1 week after the final injection (Table 1).

Improvement in time required to walk 10 m and down a flight of stairs

In the 10 ambulatory patients, except 2 and 11 who could not perform the test because of high-grade OMDS score, the time required to walk 10 m was significantly reduced from 14.7 (SE 2.6) s at commencement of PPS treatment to 12.7 s (SE 2.6) at 1 week after the final injection and 13.2 s (SE 2.6) at 5 weeks after the final injection ($p=0.017$ and $p=0.011$, respectively). The reduction rate in the time required to walk 10 m increased gradually from the commencement of treatment until 1 week after the final injection and was 14.2 % (SE 3.2) at that point. The reduction rate was 12.0 % (SE 2.3) even at 5 weeks after the final injection. These values were significant compared with the time required to walk 10 m at the commencement of treatment ($p=0.003$ and $p=0.015$, respectively) (Fig. 1a).

In the eight patients, except 2, 4, 6 and 11 who were not able to perform the test because of high-grade OMDS score, the time required to walk down a flight of stairs was also significantly reduced from 9.3 s (SE 2.0) at the commencement of treatment to 7.6 s (SE 1.6) at 1 week after the final injection, and 8.5 s (SE 2.1) at 5 weeks after the final injection ($p=0.018$ and $p=0.035$, respectively). The reduction rate in the time required to walk down a flight of stairs gradually increased from the commencement of treatment until 1 week after the final injection and was 15.4 % (SE 3.6) at that point. Although the reduction rate at 5 weeks after the final injection [10.8 % (SE 2.9)] only showed a tendency to be increased compared with the time required at the commencement of treatment ($p=0.054$), the value at 1 week after the final injection was significant compared with the time required at the commencement of treatment ($p=0.003$) (Fig. 1b).

Change in HTLV-I proviral copy number in PBMCs

PPS might have the potential to inhibit intercellular spread of HTLV-I. Therefore, before clinical trial with PPS, we

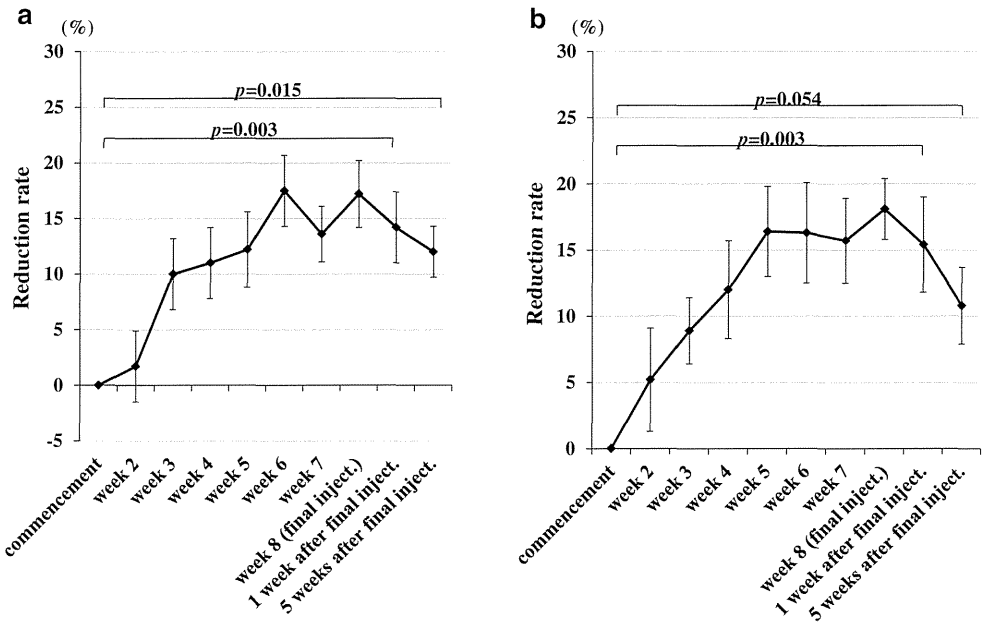

Fig. 1 Reduction rate in time required for HAM/TSP patients to walk 10 m and down a flight of stairs. **a** The reduction rate increased gradually from the commencement of treatment and was 14.2 % (SE 3.2) and 12.0 % (SE 2.3) at 1 and 5 weeks after the final injection, respectively. These values were significant compared with the time required at the commencement of treatment. **b** The reduction rate in time required to walk down a flight of stairs increased gradually from commencement of treatment and was 15.4 % (SE 3.6) and 10.8 % (SE 2.9) at 1 and 5 weeks after the final injection, respectively. Although the value at 5 weeks after the final injection only showed a tendency to increase compared with the commencement of treatment, the value at 1 week after the final injection was significant compared with the commencement of treatment. Data were analyzed using the Wilcoxon signed-rank or Kruskal–Wallis test. If significance was detected, Steel's test for post hoc comparison was performed to compare the effect of treatment with the data at the commencement of treatment. inject.=injection

investigated whether or not PPS has its activity using co-cultivation of HCT-5 with H9/K30 *luc* reporter cells in vitro. The relative luc activity significantly decreased in a dose-dependent manner, suggesting that PPS can inhibit intercellular spread of HTLV-I (Fig. 2). From this data, we expected that PPS treatment would induce the decrease of HTLV-I proviral copy number in PBMCs. Indeed, the decrease of HTLV-I proviral copy number ranged from 0.6 to 44.7 % was observed at 1 week after the final injection in cases 1–9 (Fig. 3a). However, the decrease of it was not observed at 1 week after the final injection in cases 10–12 (Fig. 3a). Overall, HTLV-I proviral copy number in PBMCs was 1,268 (SE 186), 1,156 (SE 148), 1,153 (SE 176), and 1,241 (SE 200) per 10^4 PBMCs at the commencement of treatment, treatment week 3, 1 week after the final injection, and 5 weeks after the final injection, respectively (Fig. 3b). Although the HTLV-I proviral copy number at 1 week after the final injection was decreased by about 9 % compared with that at the commencement of treatment, the decrease in HTLV-I proviral copy number at each point compared with at the commencement of treatment did not reach statistical significance.

Change in serum soluble adhesion molecules and chemokines

An increase of serum sVCAM-1 level ranged from 1 to 87.9 % was observed at 1 week after the final injection in all 12 patients. As shown in Fig. 4a, serum level of sVCAM-1 was 587 (SE 81.4), 615.8 (SE 91.5), 762.2 (SE 118.6), and 757 ng/ml (SE 127.3) at the commencement of treatment, treatment week 3, 1 week after the final injection, and 5 weeks after the final injection, respectively. It was significantly increased at 1 week after the final injection and 5 weeks after the

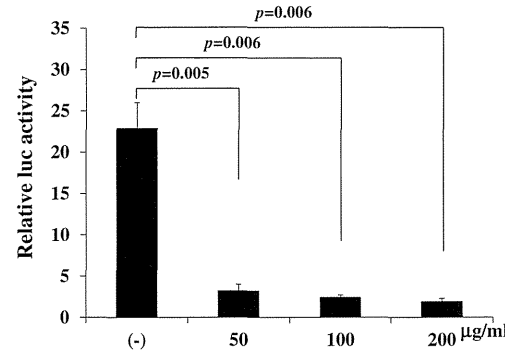

Fig. 2 The inhibitory effect for the intercellular spread of HTLV-I by PPS in vitro treatment. HCT-5 (5×10^5 cells) were co-cultivated in the presence of various concentrations of PPS with H9/K30 *luc* reporter cells (3.5×10^5 cells) in 24-well culture plate at 37 °C under 5 % CO_2. After co-cultivation for 24 h, luciferase activity was assessed by using a luciferase assay. The relative luc activity significantly decreased in a dose-dependent manner. The relative luc activity was calculated according to the following formula: relative luminescent units (RLU) of co-cultivated sample/RLU of the H9-only-cultivated sample. Data were expressed as mean±SD of triplicate cultures. Data were analyzed using Student's *t* tests

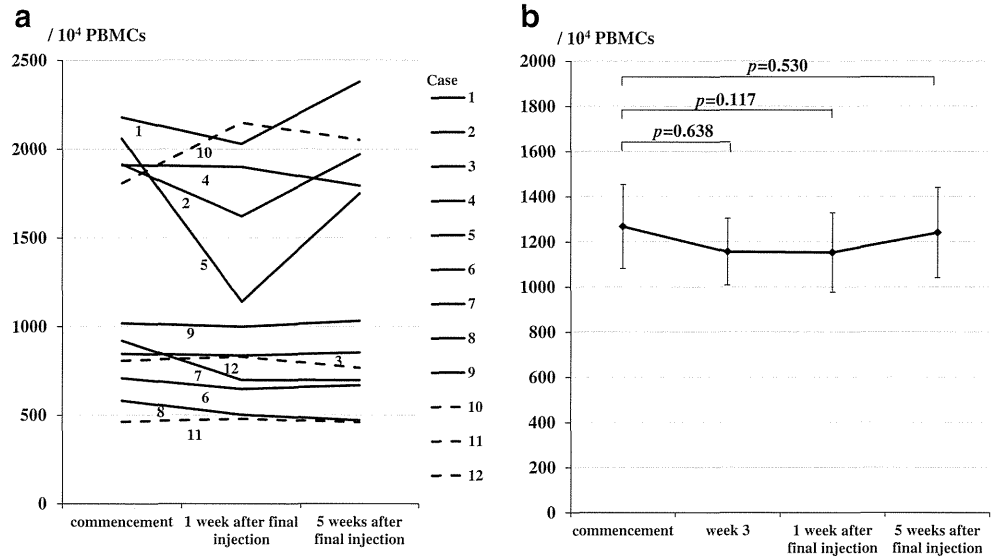

Fig. 3 Change in HTLV-I proviral copy numbers in PBMCs. **a** Changes in HTLV-I proviral copy numbers per 10^4 PBMCs at 1 week after the final injection in each case. The decrease of HTLV-I proviral copy number ranged from 0.6 to 44.7 % was observed at in cases 1–9 (indicated as *line*). However, the decrease of it was not observed in cases 10–12 (indicated as *dotted line*). **b** HTLV-I proviral copy numbers per 10^4 PBMCs were 1,268 (SE 186), 1,156 (SE 148), 1,153 (SE 176), and 1,241 (SE 200) at the commencement of treatment, treatment week 3, 1 week after the final injection, and 5 weeks after the final injection, respectively. The decrease in HTLV-I proviral copy number at each point was not significant compared with that at commencement of treatment. Data were analyzed using the Wilcoxon signed-rank test

final injection (p=0.002 and 0.015 vs the commencement of treatment, respectively). Serum level of sICAM-1 was 185.3 (SE 23.3), 184.4 (SE 23.8), 207.1 (SE 28), and 204.6 ng/ml (SE 24.9) at the commencement of treatment, treatment week 3, 1 week after the final injection, and 5 weeks after the final injection, respectively. Although the increase did not reach statistical significance, a slight trend towards an increase was observed at 1 and 5 weeks after the final injection (p=0.060 and 0.050 vs the commencement of treatment, respectively) (Fig. 4b). Serum level of CXCL10 was 209.8 (SE 56.9), 247.6 (SE 67.7), 186.2 (SE 47.3), and 242.7 pg/ml (SE 76.7) at the commencement of treatment, treatment week 3, 1 week after the final injection, and 5 weeks after the final injection, respectively. Serum level of CCL2 was 736.5 (SE 50.5), 751.1 (SE 56.0), 738.3 (SE 51.5), and 762.8 pg/ml (SE 55.4) at the commencement of treatment, treatment week 3, 1 week after the final injection, and 5 weeks after the final injection, respectively. Thus, there were no significant changes in serum levels of these two chemokines during PPS treatment (Fig. 4c, d).

Correlation between increase in sVCAM-1 and reduction in time required to walk 10 m

We evaluated the relationship between percentage increase in serum sVCAM-1 level and percentage reduction in time required to walk 10 m at 1 week after the final injection, compared with at commencement of treatment. As shown in Fig. 5, there was a moderately positive correlation between them (rs=0.648, p=0.043).

Adverse effects

All patients had a small amount of subcutaneous bleeding at the injection site. In coagulation studies 1 h after administration, the highest values were 177 s and 1.22 in ACT and PT-INR, respectively. For APTT, the highest value was 63.3 s. In blood and biochemical analyses, abnormal findings were not observed. Overall, no serious adverse effects were experienced by the HAM/TSP patients upon treatment with PPS.

Discussion

We demonstrated that PPS treatment safely improves motor disability by decreasing spasticity in the lower extremities of patients with HAM/TSP. Considering the relatively long (~21 years) mean duration of illness of the 10 ambulatory patients in our study, the efficacy of PPS treatment is a particularly interesting outcome. These results suggest that the pathological processes in the spinal cord of HAM/TSP patients is partially reversed and is treatable even if the tissues are damaged over a long period of time. We previously reported the therapeutic efficacy of heparin in HAM/TSP patients (Nagasato et al. 1993). However, we did not test whether heparin could provide safe and effective long-term treatment of HAM/TSP. Therefore, we conducted the present clinical trial with the heparinoid, PPS, the safety of which is established in Europe and the USA, even for long-term administration. The present study confirmed that PPS treatment induces effects similar to those of heparin.

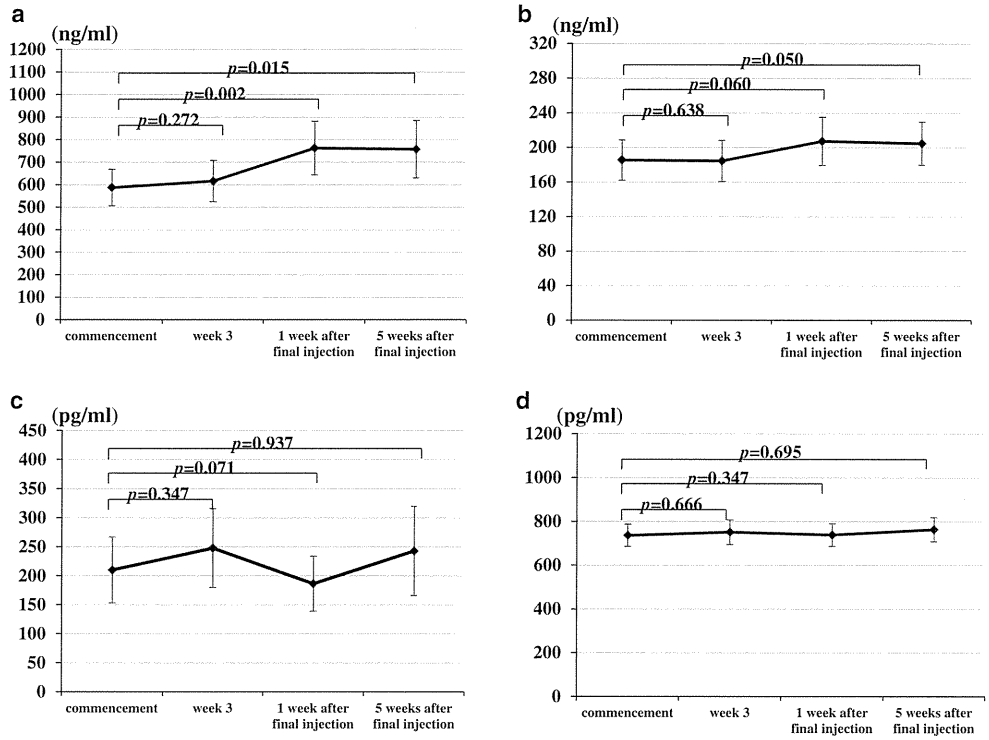

Fig. 4 Change in serum levels of sVCAM-1 and sICAM-1 and CXCL10 and CCL2. **a** Serum level of sVCAM-1 was 587 (SE 81.4), 615.8 (SE 91.5), 762.2 (SE 118.6), and 757 ng/ml (SE 127.3) at the commencement of treatment, treatment week 3, 1 week after the final injection, and 5 weeks after the final injection, respectively. It was significantly increased at 1 and 5 weeks after the final injection (p=0.002 and 0.015, vs the commencement of treatment, respectively). **b** Serum level of sICAM-1 was 185.3 (SE 23.3), 184.4 (SE 23.8), 207.1 (SE 28), and 204.6 ng/ml (SE 24.9) at the commencement of treatment, treatment week 3, 1 week after the final injection, and 5 weeks after the final injection, respectively. Although the increase did not reach significance, a slight trend towards an increase was observed at 1 and 5 weeks after the final injection (p=0.060 and 0.050, vs the commencement of treatment, respectively) (Fig. 3b). **c**, **d** There were no significant changes in serum levels of CXCL10 and CCL2 during PPS treatment. Statistical significance was determined by the Wilcoxon signed-rank test

We expected that PPS treatment would decrease the number of HTLV-I-infected cells in PBMCs through its function as a polyanion (Ida et al. 1994; Jones et al. 2005; Araya et al. 2011). Indeed, the decrease of HTLV-I proviral copy number was observed at 1 week after the final injection in 9 cases, suggesting that the intercellular spread of HTLV-I was partially blocked by PPS treatment even in vivo in these cases. However, the decrease of it was not observed at 1 week after the final injection in another 3 cases. Totally, the decrease in HTLV-I proviral copy number did not reach statistical significance in this study. This finding suggests a limitation of the protocol used in the present study. Alternatively, HTLV-I proviral load in PBMCs in HTLV-I-infected individuals including HAM/TSP patients might be mainly maintained by the proliferation of HTLV-I-infected cells (Wattel et al. 1995).

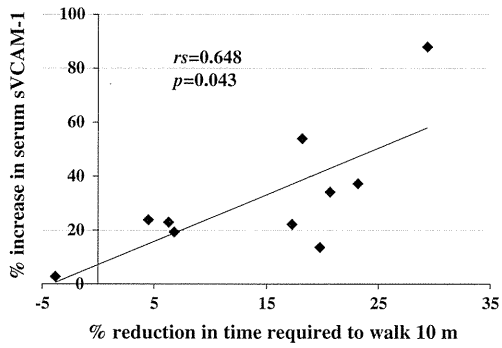

Fig. 5 Positive correlation between percentage increase in sVCAM-1 and percentage reduction in time required to walk 10 m at 1 week after the final injection compared with at commencement of treatment. There was a moderately positive correlation between them (rs=0.648, p=0.043). Correlation analysis was performed by use of nonparametric Spearman's rank correlation test

However, we demonstrated that serum levels of sVCAM-1 during treatment were significantly increased compared with pretreatment values, with a slight trend for sICAM-1 to increase. Calabresi et al. (1997) previously reported an increase in serum sVCAM-1 in MS patients treated with IFNβ-1b, which was correlated with a decrease in the number of contrast-enhancing lesions on magnetic resonance imaging. Moreover, Kallmann et al. (2000) also showed that preincubation of PBMCs with sVCAM-1 blocked their adhesion to human cerebral ECs in vitro. These results strongly suggest that sVCAM-1 can operate on very late antigen-4

(VLA-4), which is the ligand for VCAM-1, on the surface of lymphocytes as a bioactive antagonist. However, the biological functions of soluble adhesion molecules have not been entirely elucidated. It was previously reported that serum level of sVCAM-1, sICAM-1, and CXCL10 was increased, but CCL2 level was decreased, based on the immune-activated status of HAM/TSP patients (Matsuda et al. 1995; Tsukada et al. 1993; Best et al. 2006; Guerreiro et al. 2006). The precise mechanism of how serum sVCAM-1 level is increased by PPS treatment was not clear in the present study. However, there were no significant changes in serum levels of chemokines such as CXCL10 and CCL2, which is Th1-associated and Th2-associated chemokine, respectively (Best et al. 2006; Guerreiro et al. 2006), during PPS treatment. Therefore, PPS treatment does not appear to exacerbate the immune-activated status in HAM/TSP patients. We showed a correlation between the increase in sVCAM-1 and the reduction in the time required to walk 10 m at 1 week after the final injection compared with at commencement of treatment. Thus, the improvement in lower extremity motor function in HAM/TSP patients by PPS might depend on inhibition of transmigration of HTLV-I-infected cells or activated T cells inducing an inflammatory status in the lower thoracic spinal cord. Previously, an immuno-histopathological analysis in the spinal cord of HAM/TSP patients revealed that VCAM-1/VLA-4 interaction may play an important role for lymphocyte migration into the tissues (Umehara et al. 1996). In addition, as mentioned above, the main pathological regions in the central nervous tissues of HAM/TSP patients are anatomical watershed zones which lead to a slow blood flow (Izumo et al. 1989; Aye et al. 2000). Therefore, it is strongly suggested that the improvement in lower extremity motor function in HAM/TSP patients by PPS is mediated through blocking the adhesion cascade, which leads to trafficking into the tissues, by increased serum sVCAM-1 and rheological improvement of the microcirculation in the spinal cord. However, in order to confirm it, we need further analyses in the cerebrospinal fluid samples such as the changes of HTLV-I proviral load, inflammatory cytokines/chemokines, neopterin, etc. Very recently, Ando et al. (2013) clearly demonstrated that chronic inflammation in the spinal cord of HAM/TSP patients is induced by transmigration of HTLV-I-infected cells or activated T cells to the nervous tissues through CXCL10–CXCR3 inflammatory positive feedback loop. In the case of PPS treatment, this positive feedback loop might be attenuated by the inhibition of transmigration process of these cells by an increase of sVCAM-1 in the sera.

In conclusion, our results suggest that PPS, which is well tolerated in long-term administration, has the potential to be a new therapeutic tool for the treatment of HAM/TSP. Therefore, further studies are warranted to evaluate the efficacy of PPS treatment of HAM/TSP in a large randomized controlled study.

Acknowledgement We thank Prof. Akio Adachi of the University of Tokushima Graduate School for providing H9/K30 *luc* cells. We also thank the other members of the Pentosan Study Group at Nagasaki University for their suggestions at research discussions regarding the style of translational research. We are grateful to H. Benend (bene GmbH, Munich, Germany) for supplying the pentosan polysulfate SP 54 ampules and Tadashi Matsumoto (ReqMed Co., Ltd., Tokyo, Japan) for the assistance in planning this study. We would also like to acknowledge the nurses who supported this work and Kaori Furukawa for providing excellent technical assistance. This study was supported by a grant from the feasibility study stage of the Japan Science and Technology Agency (JST) (grant number AS2211341G) and partially supported by the Health and Labour Sciences Research Grant on Intractable Diseases (Neuroimmunological Diseases) from the Ministry of Health, Labour and Welfare of Japan.

Conflict of interest The authors declare that they have no conflict of interest.

References

Ando H, Sato T, Tomaru U, Yoshida M, Utsunomiya A, Yamauchi J, Araya N, Yagishita N, Coler-Reilly A, Shimizu Y, Yudoh K, Hasegawa Y, Nishioka K, Nakajima T, Jacobson S, Yamano Y (2013) Positive feedback loop via astrocytes causes chronic inflammation in virus-associated myelopathy. Brain 136:2876–2887

Araya N, Takahashi K, Sato T, Nakamura T, Sawa C, Hasegawa D, Ando H, Aratani S, Yagishita N, Fujii R, Oka H, Nishioka K, Nakajima T, Mori N, Yamano Y (2011) Fucoidan therapy decreases the proviral load in patients with human T-lymphotropic virus type-1-associated neurological disease. Antivir Ther 16:89–98

Aye MM, Matsuoka E, Moritoyo T, Umehara F, Suehara M, Hokezu Y, Yamanaka H, Isashiki Y, Osame M, Izumo S (2000) Histopathological analysis of four autopsy cases of HTLV-I-associated myelopathy/tropical spastic paraparesis: inflammatory changes occur simultaneously in the entire central nervous system. Acta Neuropathol 100:245–252

Best I, Adaui V, Verdonck K, González E, Tipismana M, Clark D, Gotuzzo E, Vanham G (2006) Proviral load and immune markers associated with human T-lymphotropic virus type 1 (HTLV-1)-associated myelopathy/tropical spastic paraparesis (HAM/TSP) in Peru. Clin Exp Immunol 146:226–233

Bohannon RW, Smith MB (1987) Interrater reliability of a modified Ashworth scale of muscle spasticity. Phys Ther 67:206–207

Calabresi PA, Tranquill LR, Dambrosia JM, Stone LA, Maloni H, Bash CN, Frank JA, McFarland HF (1997) Increases in soluble VCAM- I correlate with a decrease in MRI lesions in multiple sclerosis treated with interferon β-I b. Ann Neurol 41:669–674

de-Thé G, Bomford R (1993) An HTLV-I vaccine: why, how, for whom? AIDS Res Hum Retroviruses 9:381–386

Fukushima N, Nakamura T, Nishiura Y, Ida H, Aramaki T, Eguchi K (2008) HTLV-I production based on activation of integrin/ligand signaling in HTLV-I-infected T cell lines derived from HAM/TSP patients. Intervirology 51:1234–1239

Ghosh P (1999) The pathobiology of osteoarthritis and the rationale for the use of pentosan polysulfate for its treatment. Semin Arthritis Rheum 28:211–267

Guerreiro JB, Santos SB, Morgan DJ, Porto AF, Muniz AL, Ho JL, Teixeira AL Jr, Teixeira MM, Carvalho EM (2006) Levels of serum chemokines discriminate clinical myelopathy associated with human T lymphotropic virus type 1 (HTLV-1)/tropical spastic paraparesis (HAM/TSP) disease from HTLV-1 carrier state. Clin Exp Immunol 145:296–301

Hollsberg P, Hafler DA (1993) Pathogenesis of diseases induced by human T-lymphotropic virus type I infection. N Engl J Med 328:1173–1182

Ida H, Kurata A, Eguchi K, Yamashita I, Nakashima M, Sakai M, Kawabe Y, Nakamura T, Nagataki S (1994) Mechanism of inhibitory effect of dextran sulfate and heparin on human T-cell lymphotropic virus type I (HTLV-I)-induced syncytium formation in vitro: role of cell to cell contact. Antiviral Res 23:143–159

Igakura T, Stinchcombe JC, Goon PK, Taylor GP, Weber JN, Griffiths GM, Tanaka Y, Osame M, Bangham CR (2003) Spread of HTLV-I between lymphocytes by virus-induced polarization of the cytoskeleton. Science 299:1713–1716

Ijichi S, Izumo S, Eiraku N, Machigashira K, Kubota R, Nagai M, Ikegami N, Kashio N, Umehara F, Maruyama I, Osame M (1993) An autoaggressive process against bystander tissues in HTLV-I-infected individuals: a possible pathomechanism of HAM/TSP. Med Hypotheses 41:542–547

Irony-Tur-Sinai M, Vlodavsky I, Ben-Sasson SA, Pinto F, Sicsic C, Brenner T (2003) A synthetic heparin-mimicking polyanionic compound inhibits central nervous system inflammation. J Neurol Sci 206:49–57

Izumo S, Usuku K, Osame M, Machigashira K, Johnosono M, Nakagawa M (1989) The neuropathology of HLV-I-associated myelopathy in Japan: report of an autopsy case and review of the literature. In: Román GC, Vernant J-C, Osame M (eds) HTLV-I and the nervous system. Alan R, Liss, Inc, New York, pp 261–267

Jones KS, Petrow-Sadowski C, Bertolette DC, Huang Y, Ruscetti FW (2005) Heparan sulfate proteoglycans mediate attachment and entry of human T-cell leukemia virus type 1 virions into CD4+ T cells. J Virol 79:12692–12702

Kallmann BA, Hummel V, Lindenlaub T, Ruprecht K, Toyka KV, Rieckmann P (2000) Cytokine-induced modulation of cellular adhesion to human cerebral endothelial cells is mediated by soluble vascular cell adhesion molecule-1. Brain 123:687–697

Kumagai K, Shirabe S, Miyata N, Murata M, Yamauchi A, Kataoka Y, Niwa M (2010) Sodium pentosan polysulfate resulted in cartilage improvement in knee osteoarthritis—an open clinical trial. BMC Clin Pharma 10:7

Matsuda M, Tsukada N, Miyagi K, Yanagisawa N (1995) Increased levels of soluble vascular cell adhesion molecule-l (VCAM-1) in the cerebrospinal fluid and sera of patients with multiple sclerosis and human T lymphotropic virus type-1-associated myelopathy. J Neuroimmunol 59:35–40

Nagasato K, Nakamura T, Ichinose K, Nishiura Y, Ohishi K, Shibayama K, Watanabe H, Tsujihata M, Nagataki S (1993) Heparin treatment in patients with human T-lymphotropic virus type I (HTLV-I)-associated myelopathy. J Neurol Sci 115:161–168

Nakamura T, Nishiura Y, Eguchi K (2009) Therapeutic strategies in HTLV-I-associated myelopathy/tropical spastic paraparesis (HAM/TSP). Cent Nerv Syst Agents Med Chem 9:137–149

Nakamura T (2009) HTLV-I-associated myelopathy/tropical spastic paraparesis (HAM/TSP): the role of HTLV-I-infected Th1 cells in the pathogenesis, and therapeutic strategy. Folia Neuropathol 47: 182–194

Nishiura Y, Nakamura T, Fukushima N, Nakamura H, Ida H, Aramaki T, Eguchi K (2009) Disulfide-mediated apoptosis of human T-lymphotropic virus type-I (HTLV-I)-infected cells in patients with HTLV-I-associated myelopathy/tropical spastic paraparesis. Antivir Ther 14:533–542

Osame M, Matsumoto M, Usuku K, Izumo S, Ijichi N, Amitani H, Tara M, Igata A (1987) Chronic progressive myelopathy associated with elevated antibodies to human T-lymphotropic virus type I and adult T-cell leukemia-like cells. Ann Neurol 21: 117–122

Osame M, Igata A, Matsumoto M (1989) HTLV-I-associated myelopathy (HAM) revisited. In: Román GC, Vernant J-C, Osame M (eds) HTLV-I and the nervous system. Alan R, Liss, Inc, New York, pp 213–223

Osame M (1990) Review of WHO Kagoshima meeting and diagnostic guidelines for HAM/TSP. In: Blattner WA (ed) Human retrovirology: HTLV. Raven, New York, pp 191–197

Tsukada N, Miyagi K, Matsuda M, Yanagisawa N (1993) Increased levels of circulating intercellular adhesion molecule-1 in multiple sclerosis and human T-lymphotropic virus type I-associated myelopathy. Ann Neurol 33:646–649

Umehara F, Izumo S, Takeya M, Takahashi K, Sato E, Osame M (1996) Expression of adhesion molecules and monocyte chemoattractant protein-1 (MCP-1) in the spinal cord lesions in HTLV-I-associated myelopathy. Acta Neuropathol 91:343–350

Wattel E, Vartanian JP, Pannetier C, Wain-Hobson S (1995) Clonal expansion of human T-cell leukemia virus type I-infected cells in asymptomatic and symptomatic carriers without malignancy. J Virol 69:2863–2868

Weiner HL, Hafler DA (1988) Immunotherapy of multiple sclerosis. Ann Neurol 23:211–222

Yoshida A, Piroozmand A, Sakurai A, Fujita M, Uchiyama T, Kimura T, Hayashi Y, Kiso Y, Adachi A (2005) Establishment of a biological assay system for human retroviral protease activity. Microbes Infect 7:820–824

OPEN ACCESS Freely available online

PLOS ONE

Familial Clusters of HTLV-1-Associated Myelopathy/Tropical Spastic Paraparesis

Satoshi Nozuma[1], Eiji Matsuura[1]*, Toshio Matsuzaki[2], Osamu Watanabe[1], Ryuji Kubota[2], Shuji Izumo[2], Hiroshi Takashima[1]

1 Department of Neurology and Geriatrics, Kagoshima University Graduate School of Medical and Dental Sciences, Kagoshima city, Japan, **2** Department of Molecular Pathology, Center for Chronic Viral Diseases, Kagoshima University Graduate School of Medical and Dental Sciences, Kagoshima city, Japan

Abstract

Objective: HTLV-1 proviral loads (PVLs) and some genetic factors are reported to be associated with the development of HTLV-1-associated myelopathy/tropical spastic paraparesis (HAM/TSP). However, there are very few reports on HAM/TSP having family history. We aimed to define the clinical features and laboratory indications associated with HAM/TSP having family history.

Methods: Records of 784 HAM/TSP patients who were hospitalized in Kagoshima University Hospital and related hospitals from 1987 to 2012 were reviewed. Using an unmatched case-control design, 40 patients of HAM/TSP having family history (f-HAM/TSP) were compared with 124 patients suffering from sporadic HAM/TSP, who were admitted in series over the last 10 years for associated clinical features.

Results: Of the 784 patients, 40 (5.1%) were f-HAM/TSP cases. Compared with sporadic cases, the age of onset was earlier (41.3 vs. 51.6 years, $p<0.001$), motor disability grades were lower (4.0 vs. 4.9, $p=0.043$) despite longer duration of illness (14.3 vs. 10.2 years, $p=0.026$), time elapsed between onset and wheelchair use in daily life was longer (18.3 vs. 10.0 years, $p=0.025$), cases with rapid disease progression were fewer (10.0% vs. 28.2%, $p=0.019$), and protein levels in cerebrospinal fluid (CSF) were significantly lower in f-HAM/TSP cases (29.9 vs. 42.5 mg, $p<0.001$). There was no difference in HTLV-1 PVLs, anti-HTLV-1 antibody titers in serum and CSF, or cell number and neopterin levels in CSF. Furthermore, HTLV-1 PVLs were lower in cases with rapid disease progression than in those with slow progression in both f-HAM/TSP and sporadic cases.

Conclusions: We demonstrated that HAM/TSP aggregates in the family, with a younger age of onset and a slow rate of progression in f-HAM/TSP cases compared with sporadic cases. These data also suggested that factors other than HTLV-1 PVLs contribute to the disease course of HAM/TSP.

Citation: Nozuma S, Matsuura E, Matsuzaki T, Watanabe O, Kubota R, et al. (2014) Familial Clusters of HTLV-1-Associated Myelopathy/Tropical Spastic Paraparesis. PLoS ONE 9(5): e86144. doi:10.1371/journal.pone.0086144

Editor: Steven Jacobson, National Institutes of Health, United States of America

Received June 6, 2013; **Accepted** December 5, 2013; **Published** May 6, 2014

Funding: This study was supported by Health and Labour Sciences Research Grants from the Ministry of Health Labour and Welfare and JSPS KAKENHI Grant Numbers 25293205 and 24133701. The funders had no role in study design, data collection and analysis, decision to publish, or preparation of the manuscript.

Competing Interests: The authors have declared that no competing interests exist.

* E-mail: pine@m.kufm.kagoshima-u.ac.jp

Introduction

HTLV-1-associated myelopathy/tropical spastic paraparesis (HAM/TSP) is characterized by slow progressive spastic paraparesis and positivity for anti-HTLV-1 antibodies in both serum and cerebrospinal fluid (CSF) [1,2]. Worldwide, at least 10–20 million people are infected with HTLV-1 [3]. However, although the majority of infected individuals remain lifelong asymptomatic carriers, approximately 2%–5% develop adult T-cell lymphomas [4,5] and another 0.25%–3.8% develop HAM/TSP [1,2]. Although the mechanisms underlying the development of HAM/TSP are not fully understood, several risk factors are closely associated with HAM/TSP. In particular, HTLV-1 proviral loads (PVLs) are significantly higher in HAM/TSP patients than in asymptomatic carriers and are also higher in genetic relatives of HAM/TSP patients than in non-HAM-related asymptomatic carriers [6]. Host genetic factors, including human leukocyte antigen (HLA) and non-HLA gene polymorphisms affect the occurrence of HAM/TSP [7], indicating that HTLV-1 PVLs and genetic backgrounds may influence individual susceptibility to HAM/TSP. Although several reports of familial adult T-cell lymphoma have been published [8,9], to our knowledge, there is only one case report of patient with HAM/TSP having family history (f-HAM/TSP) [10]. Hence, little is known about the prevalence and character of f-HAM/TSP cases. In this study, the characteristic clinical and laboratory features of f-HAM/TSP cases are defined and compared with those of sporadic cases.

Methods

Ethics Statement

This study was approved by the Institutional Review Boards of Kagoshima University. All participants provided written informed consent.

Design

We used an unmatched case-control design to identify the phenotypic features of f-HAM/TSP. f-HAM/TSP cases were identified as patients with multiple family members suffering from HAM/TSP. Controls were defined as HAM/TSP patients who were not genetically related to other HAM/TSP patients.

Subjects

f-HAM/TSP cases were extracted from our database of individuals diagnosed with HAM/TSP in Kagoshima University Hospital and related hospitals from 1987 to 2012. Controls included consecutive patients with sporadic HAM/TSP who were evaluated in our department between January 2002 and June 2012. HAM/TSP was diagnosed according to the World Health Organization diagnostic criteria, and the updated criteria of Castro-costa Belem [11]. Clinical information was obtained from the medical records of patient attendance at our hospital. In other cases, clinical data were obtained from the clinical records of patients or directly from the referring clinicians. Clinical variables included sex, age, age of onset, and initial symptoms. Neurological disabilities were assessed using Motor Disability Grading (MDG), modified from the Osame Motor Disability Scale of 0 to 10, as reported previously [12]. Motor disability grades were defined as follows: 5, needs one-hand support while walking; 6, needs two-hand support while walking; and 7, unable to walk but can crawl. We used a different assessment for the subgroup of more than grade 6 because their disease state significantly interfered with their lifestyle and necessitated the use of wheelchairs in daily life. The subgroup of patients with rapid progression was defined by deterioration of motor disability by more than three grades within two years. Anti-HTLV-1 antibody titers in serum and CSF were detected using enzyme-linked immunosorbent assays and particle agglutination methods (Fijirebio Inc, Tokyo, Japan). HTLV-1 PVLs in peripheral blood mononuclear cells (PBMCs) were assayed using quantitative PCR with the ABI PRISM 7700TM sequence detection system as reported previously [6].

Statistical Analysis

Data were analyzed using SPSS-20 (SPSS, Chicago, Illinois). Statistical analyses were performed using parametric (t-test) and non-parametric tests (Mann–Whitney test) for continuous variables and χ^2 (Pearsonχ^2 test/Fisher exact test) for categorical variables. Significant differences were then adjusted for potential confounders (age and sex) using multiple linear regression analysis. Survival was estimated according to the Kaplan–Meier method. The final endpoint was defined by a MDG score of 6. Patients with MDG scores of 6 almost wheelchair bound in daily life. The log rank test was used in Kaplan–Meier analyses. Differences were considered significant when $p<0.05$.

Results

Clinical characteristics of f-HAM/TSP

Of the 784 patients diagnosed with HAM/TSP between January 1987 and June 2012, 40 (5.1%) were f-HAM/TSP. The sex ratio was 33 males : 7 females. Of these 40 cases, 10 had parents or children (25.0%), 27 had siblings (67.5%), and three had other relatives (7.5%) diagnosed with HAM/TSP. Three individuals from one family were diagnosed with HAM/TSP, whereas only two individuals were diagnosed with HAM/TSP in all other families. In f-HAM/TSP cases, the age of onset was earlier (41.3 vs. 51.6 years, $p<0.001$), cases with rapid progression were fewer (10.0% vs. 28.2%, $p = 0.019$), motor disability grades were lower (4.0 vs. 4.9, $p = 0.043$) despite longer duration of illness (14.3 vs. 10.2 years, $p = 0.026$), and time elapsed between onset and wheelchair use in daily life was longer (18.3 vs. 10.0 years, $p = 0.025$) compared with sporadic cases. Sex and initial symptoms did not differ significantly between f-HAM/TSP and sporadic cases (Table 1). Twelve patients of f-HAM/TSP, and 38 of the 128 sporadic cases reached endpoint MDG scores of 6. Significant differences were then adjusted for potential confounders (age and sex) using multivariate analysis. Age of onset, duration of illness, MDG scores, and time elapsed between onset and wheelchair use in daily life remained significantly different after multivariate analysis (Table 1). The proportion of patients with rapid progression did not differ significantly between the groups, although there was a trend toward a higher proportion in sporadic cases. Kaplan–Meier analyses revealed that approximately 30% of both f-HAM/TSP and sporadic cases needed a wheelchair in daily life in 15 years after onset, and approximately 50% of patients from both groups needed it in 20 years after onset (Figure 1). Although sporadic patients needed wheelchairs earlier in most cases, the difference in the ratio of the patients with MDG score above six was not statistically significant between the groups. Finally, we compared differences in the age of onset between parent–child and sibling cases in f-HAM/TSP cases. Age of onset in parent–child f-HAM/TSP cases was significantly younger than that in sibling f-HAM/TSP cases (29.9 ± 10.0 vs. 45.1 ± 13.0 years, $p = 0.002$).

Laboratory parameters and PVLs in f-HAM/TSP cases

Protein levels in CSF were significantly lower in f-HAM/TSP cases than in sporadic cases (29.9 vs. 42.5 mg/dl, $p<0.001$). This difference in CSF protein level remained significant after multivariate analysis. Anti-HTLV-1 antibody titers in serum and CSF, and cell numbers and neopterin levels in CSF were not significantly different between two groups. Moreover, HTLV-1 PVLs did not differ significantly. (Table 2).

Clinical and laboratory findings in patients with rapid disease progression

Previous studies suggest that an older age of onset is associated with rapid disease progression. Similar findings are found in the present study. The percentage of rapid progression tended to increase with older age of onset in both f-HAM/TSP and sporadic groups (Figure 2). We compared the characteristics of 124 sporadic HAM/TSP patients with rapid and slow progression who were admitted to Kagoshima University Hospital in series during the last 10 years (Table 3). Patients with rapid progression were significantly older at onset than those with slow progression (62.3 vs. 47.4 years, $p<0.001$), although sex and initial symptoms did not differ significantly between rapid and slow progression groups. However, the time elapsed between onset and wheelchair use in daily life was markedly shorter among patients with rapid progression (1.5 vs. 14.4 years, $p<0.001$). Cell numbers, protein levels, and anti-HTLV-1 antibody titers in CSF were significantly higher in patients with rapid progression than in those with slow progression (11.6 vs. 3.2, $p<0.001$; 55.3 vs. 36.7 mg/dl, $p<0.001$; 1,251 vs. 416, $p<0.014$, respectively). Interestingly, HTLV-1 PVLs were significantly lower in patients with rapid progression than in those with slow progression (370 vs. 1,245 copies, $p<0.001$). Furthermore, we compared the differences between women and men in patients with rapid progression because the reason remains unknown why HAM/TSP is common in female

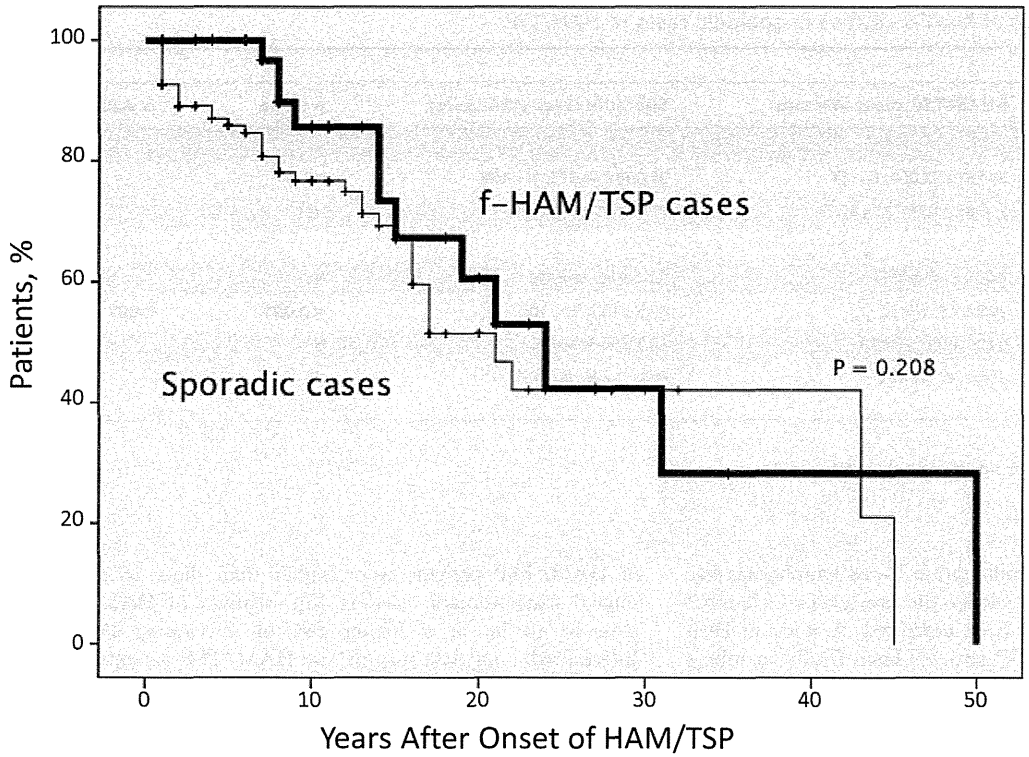

Figure 1. Kaplan–Meier estimates of the time from disease onset to assignment of motor disability scores of 6. In sporadic cases, more patients reached the score of six at an early stage; however, the difference was not significant. Approximately 30% of both f-HAM/TSP cases and sporadic cases needed a wheelchair in daily life in 15 years after onset and approximately 50% of patients from both groups needed a wheelchair in 20 years after onset.
doi:10.1371/journal.pone.0086144.g001

than in male. There was no significant difference between women and men in the age of onset (61.5 y.o.±12.6 vs. 62.7 y.o.±12.5), in the incidence of rapid progression (26.3% vs. 32.3%) and in MDG score (5.4 vs. 5.0; mean).

Discussion

We demonstrated that among 784 HAM/TSP patients, 40 (5.1%) had family members with the disease. The lifetime risk of developing HAM/TSP is 0.25% of HTLV-1 carriers in Japan

Table 1. Clinical features of f-HAM/TSP cases or sporadic cases of HAM/TSP.

	f-HAM/TSP cases (40 cases)	Sporadic cases (124 cases)	p value	p value†
Female ratio (%)	78.8% (7 males : 33 females)	66.4% (31 males : 93 females)	NS	
Age	55.6±13.0 (23–79)	61.8±12.5 (15–83)	**0.008**	
Age of onset	41.3±13.9 (14–65)	51.6±15.9 (13–78)	**<0.001**	**0.017**
Duration of illness (years)	14.3±11.4 (1–49)	10.2±9.6 (0–45)	**0.026**	**0.017**
Initial symptoms				
Gait disturbance	50.0%	52.4%	NS	
Urinary disturbance	32.5%	26.6%	NS	
Sensory disturbance	12.5%	14.5%	NS	
Others	5%	6.5%	NS	
Rapid disease progression	4 cases (10.0%)	35 cases (28.2%)	**0.019**	0.069
Motor disability score	4.0±2.0 (0–7)	4.9±1.5 (0–8)	**0.043**	**0.036**
Score more than 6	12 cases (30.0%)	38 cases (30.7%)	NS	
Time elapsed between onset and wheelchair use in daily life (years)	18.3±12.4 (7–50)	10.0±10.4 (1–45)	**0.025**	**0.020**

Data are presented as mean values ± s.d., (range),
†Adjusted for age and sex.
doi:10.1371/journal.pone.0086144.t001

Table 2. Laboratory findings of familial clusters or sporadic cases of HAM/TSP.

	f-HAM/TSP cases (40cases)	Sporadic cases (124 cases)	p value	p value†
Anti-HTLV-1 antibodies*				
Titer in Serum	20,787±31,004, N = 37	31,009±36,075, N = 109	NS	
Titer in CSF	2,310±11,741, N = 31	672±1,274, N = 111	NS	
Cerebrospinal fluid				
Cell number (/mm^3)	3.0±2.5, N = 25	5.7±10.0, N = 109	NS	
Protein (mg/dl)	29.9±9.4, N = 22	42.5±19.3, N = 109	**<0.001**	**0.007**
Neopterin (pmol/ml)	83.2±118.1, N = 18	38.3±56.8, N = 35	NS	
HTLV-1 proviral loads (Copies/10^4 PBMCs)	930±781, N = 32	968±1,746, N = 101	NS	

* Particle Aggregation Method.
Data are presented as mean values ± s.d., N = sample number,
†Adjusted for age and sex.
doi:10.1371/journal.pone.0086144.t002

[13]. Although clustering of familial adult T-cell lymphomas has been reported [8,9], to our knowledge the prevalence of familial clusters of HAM/TSP has not been described. A study in Peru showed that 30% of HAM/TSP patients have family members with paralytic neurological disorders, but the cause of paralysis was not evaluated [14]. In the present study, we included f-HAM/TSP diagnosed in medical institutions and excluded cases with a family history of neurological disorders. Thus, the actual incidence rates of f-HAM/TSP may be higher than those reported here. Interestingly, although HTLV-1 PVL has been associated with the development and clinical progression of HAM/TSP [15–17], there was no significant difference between f-HAM/TSP and sporadic cases in the present study. Because previous studies reported that HTLV-1 PVLs of asymptomatic carriers in relatives of HAM/TSP patients were higher than those in non-HAM-related asymptomatic carriers [6], relatives of HAM/TSP are believed to be at a higher risk of developing HAM/TSP. Interestingly, our data suggest that HAM/TSP patients aggregate in families and factors other than HTLV-1 PVLs may contribute to HAM/TSP.

Compared with sporadic HAM/TSP, the clinical characteristics of f-HAM/TSP have a younger age of onset and longer time elapsed between onset and wheelchair use in daily life. Although we were unable to identify the reason for earlier onset among f-HAM/TSP cases, one can speculate that mild symptoms, such as urinary and sensory disturbances, may be identified earlier by family members who are familiar with HAM/TSP symptoms. However, the present data show no difference in initial symptoms

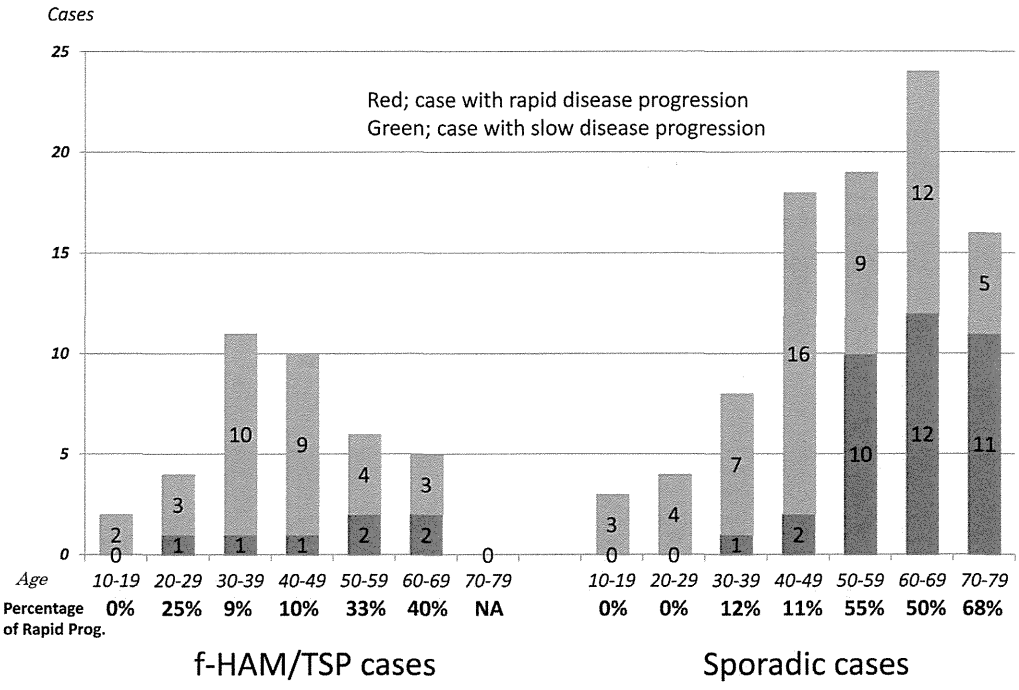

Figure 2. Age-specific proportions of rapid disease progression. The proportion of cases with rapid disease progression tended to increase with the older age of onset.
doi:10.1371/journal.pone.0086144.g002

Table 3. Clinical and laboratory findings of sporadic HAM/TSP with rapid/slow disease progression.

Type of disease progression	Rapid progression	Slow progression	p value
Female ratio (%)	71.4% (10 males : 25 females)	76.4% (21 males : 68 females)	NS
Age of onset	62.3±9.6, N=35	47.4±15.9, N=89	**<0.001**
Age of onset of f-HAM/TSP cases	60.5±3.7, N=4	39.2±12.9, N=36	**0.002**
Duration between onset and inability to walk alone (years)	1.5±0.9, N=13	14.4±10.4, N=25	**<0.001**
Anti-HTLV-1 antibodies*			
Titer in Serum	31,894±36,845, N=34	30,608±35,965, N=75	NS
Titer in CSF	1,251±1,800, N=34	416±852, N=77	**0.014**
Cerebrospinal fluid			
Cell number (/mm^3)	11.6±16.6, N=34	3.2±3.5, N=75	**<0.001**
Protein (mg/dl)	55.3±24.3, N=34	36.7±13.0, N=75	**<0.001**
Neopterin (pmol/ml)	74.9±107.9, N=8	27.4±23.4, N=27	0.255
HTLV-1 proviral loads (Copies/10^4 PBMCs)	370±327, N=32	1,245±2,046, N=69	**<0.001**

* Particle Aggregation Method.
Data are presented as mean values ± s.d., N=sample number.
doi:10.1371/journal.pone.0086144.t003

between f-HAM/TSP and sporadic cases. In all cases, the age of onset and initial symptoms of HAM/TSP were evaluated by the neurologists during hospitalization. Because inflammatory processes are less marked in f-HAM/TSP cases, as indicated by significantly lower protein levels in CSF, f-HAM/TSP cases may show slow progression of disease.

We need to discuss the possibility that the two groups compared represent different mode of HTLV transmission, i.e. vertical vs. sexual transmission. To clarify genetic backgrounds, sporadic HAM/TSP with seropositive carrier family members may be a more appropriate control, but are not available at present. The incidence of female cases showing no significant differences between f-HAM/TSP and sporadic cases, and between rapid and slow disease progression, might suggest less possibility of sporadic cases due to sexual transmission.

Although the subgroup of patients with rapid progression has not been clearly defined, previous studies suggest that rapid progression occurs in 10%–30% of all patients with HAM/TSP [12,14,16], and is associated with an older age of onset [14–16]. In the present study, the age of onset in patients with rapid progression was significantly older than that in patients with slow progression between f-HAM/TSP and sporadic cases, and the proportion of patients with rapid progression increased with the older age of onset (Figure 2). Among sporadic cases, cell numbers and protein levels in CSF were significantly higher in patients with rapid progression, suggesting that inflammation is more active in the spinal cords of patients with rapid progression and that cytotoxic T-lymphocyte (CTL) immune responses may be more intensive. Therefore, lower PVLs in PBMCs of patients with rapid disease progression may be attributed to the strong killing ability of the CTL. However, PVLs were higher in PBMCs of patients with HAM/TSP than in asymptomatic carriers [6]. In addition, the killing ability of CTLs in patients with HAM/TSP does not differ from that in asymptomatic carriers [18]. Hence, strong immune responses may be associated with the disease course. The onset of disease may require other factors that lead to strong immune responses. A late onset may also be associated with alterations of the immune function in HTLV-1-infected patients. Indeed, an increased age has been associated with autoimmune disorders, such as myasthenia gravis and rheumatoid arthritis, and may be partly explained by immune intolerance and accumulation of autoantibodies in older individuals [19,20].

In conclusion, we demonstrated that patients with HAM/TSP aggregate in some families. Compared with sporadic cases, the age of onset was younger and rates of disease progression were slower among familial cases, whereas HTLV-1 PVLs did not differ between f-HAM/TSP and sporadic groups. The present data suggest that factors other than HTLV-1 PVLs contribute to the disease course of HAM/TSP. Our data also suggested strong immune responses in the spinal cord of HAM/TSP patients with rapid progression. Further studies on HTLV-1, immune response to HTLV-1 and genetic factor in patients with rapid progression might provide new insights into HAM/TSP pathogenesis.

Acknowledgments

We would like to express the deepest appreciation to Yuka Komai for collecting information from patients and Dr. Moe Moe Aye for reading our manuscript.

Author Contributions

Conceived and designed the experiments: HT SI OW. Performed the experiments: SN EM. Analyzed the data: SN EM. Contributed reagents/materials/analysis tools: SN EM TM RK. Wrote the paper: SN EM.

References

1. Gessain A, Barin F, Vernant JC, Gout O, Maurs L, et al. (1985) Antibodies to human T-lymphotropic virus type-I in patients with tropical spastic paraparesis. Lancet 2: 407–410.
2. Osame M, Usuku K, Izumo S, Ijichi N, Amitani H, et al. (1986) HTLV-I associated myelopathy, a new clinical entity. Lancet 1: 1031–1032.
3. Proietti FA, Carneiro-Proietti AB, Catalan-Soares BC, Murphy EL (2005) Global epidemiology of HTLV-I infection and associated diseases. Oncogene 24: 6058–6068.
4. Hinuma Y, Nagata K, Hanaoka M, Nakai M, Matsumoto T, et al. (1981) Adult T-cell leukemia: antigen in an ATL cell line and detection of antibodies to the antigen in human sera. Proc Natl Acad Sci U S A 78: 6476–6480.

5. Uchiyama T, Yodoi J, Sagawa K, Takatsuki K, Uchino H (1977) Adult T-cell leukemia: clinical and hematologic features of 16 cases. Blood 50: 481–492.
6. Nagai M, Usuku K, Matsumoto W, Kodama D, Takenouchi N, et al. (1998) Analysis of HTLV-I proviral load in 202 HAM/TSP patients and 243 asymptomatic HTLV-I carriers: high proviral load strongly predisposes to HAM/TSP. J Neurovirol 4: 586–593.
7. Saito M (2010) Immunogenetics and the Pathological Mechanisms of Human T-Cell Leukemia VirusType 1- (HTLV-1-)Associated Myelopathy/Tropical Spastic Paraparesis (HAM/TSP). Interdiscip Perspect Infect Dis 2010: 478461.
8. Pombo-de-Oliveira MS, Carvalho SM, Borducchi D, Dobbin J, Salvador J, et al. (2001) Adult T-cell leukemia/lymphoma and cluster of HTLV-I associated diseases in Brazilian settings. Leuk Lymphoma 42: 135–144.
9. Miyamoto Y, Yamaguchi K, Nishimura H, Takatsuki K, Motoori T, et al. (1985) Familial adult T-cell leukemia. Cancer 55: 181–185.
10. Mori M, Ban N, Kinoshita K (1988) Familial occurrence of HTLV-I–associated myelopathy. Ann Neurol 23: 100.
11. De Castro-Costa CM, Araujo AQ, Barreto MM, Takayanagui OM, Sohler MP, et al. (2006) Proposal for diagnostic criteria of tropical spastic paraparesis/ HTLV-I-associated myelopathy (TSP/HAM). AIDS Res Hum Retroviruses 22: 931–935.
12. Nakagawa M, Izumo S, Ijichi S, Kubota H, Arimura K, et al. (1995) HTLV-I-associated myelopathy: analysis of 213 patients based on clinical features and laboratory findings. J Neurovirol 1: 50–61.
13. Kaplan JE, Osame M, Kubota H, Igata A, Nishitani H, et al. (1990) The risk of development of HTLV-I-associated myelopathy/tropical spastic paraparesis among persons infected with HTLV-I. J Acquir Immune Defic Syndr 3: 1096–1101.
14. Gotuzzo E, Cabrera J, Deza L, Verdonck K, Vandamme AM, et al. (2004) Clinical characteristics of patients in Peru with human T cell lymphotropic virus type 1-associated tropical spastic paraparesis. Clin Infect Dis 39: 939–944.
15. Matsuzaki T, Nakagawa M, Nagai M, Usuku K, Higuchi I, et al. (2001) HTLV-I proviral load correlates with progression of motor disability in HAM/TSP: analysis of 239 HAM/TSP patients including 64 patients followed up for 10 years. J Neurovirol 7: 228–234.
16. Olindo S, Cabre P, Lezin A, Merle H, Saint-Vil M, et al. (2006) Natural history of human T-lymphotropic virus 1-associated myelopathy: a 14-year follow-up study. Arch Neurol 63: 1560–1566.
17. Takenouchi N, Yamano Y, Usuku K, Osame M, Izumo S (2003) Usefulness of proviral load measurement for monitoring of disease activity in individual patients with human T-lymphotropic virus type I-associated myelopathy/ tropical spastic paraparesis. J Neurovirol 9: 29–35.
18. Asquith B, Mosley AJ, Barfield A, Marshall SE, Heaps A, et al. (2005) A functional CD8+ cell assay reveals individual variation in CD8+ cell antiviral efficacy and explains differences in human T-lymphotropic virus type 1 proviral load. J Gen Virol 86: 1515–1523.
19. Manoussakis MN, Tzioufas AG, Silis MP, Pange PJ, Goudevenos J, et al. (1987) High prevalence of anti-cardiolipin and other autoantibodies in a healthy elderly population. Clin Exp Immunol 69: 557–565.
20. Aprahamian T, Takemura Y, Goukassian D, Walsh K (2008) Ageing is associated with diminished apoptotic cell clearance in vivo. Clin Exp Immunol 152: 448–455.

J Neuropathol Exp Neurol

Vol. 74, No. 1
January 2015
pp. 2–14

ORIGINAL ARTICLE

OPEN

Visualization of HTLV-1–Specific Cytotoxic T Lymphocytes in the Spinal Cords of Patients With HTLV-1–Associated Myelopathy/Tropical Spastic Paraparesis

Eiji Matsuura, MD, PhD, Ryuji Kubota, MD, PhD, Yuetsu Tanaka, MD, PhD, Hiroshi Takashima, MD, PhD, and Shuji Izumo, MD, PhD

Abstract

Activated human T-lymphotropic virus type-1 (HTLV-1)–specific CD8-positive cytotoxic T lymphocytes (CTLs) are markedly increased in the periphery of patients with HTLV-1–associated myelopathy/tropical spastic paraparesis (HAM/TSP), an HTLV-1–induced inflammatory disease of the CNS. Although virus-specific CTLs play a pivotal role to eliminate virus-infected cells, the potential role of HTLV-1–specific CTLs in the pathogenesis of HAM/TSP remains unclear. To address this issue, we evaluated the infiltration of HTLV-1–specific CTLs and the expression of HTLV-1 proteins in the spinal cords of 3 patients with HAM/TSP. Confocal laser scanning microscopy with our unique staining procedure made it possible to visualize HTLV-1–specific CTLs infiltrating the CNS of the HAM/TSP patients. The frequency of HTLV-1–specific CTLs was more than 20% of CD8-positive cells infiltrating the CNS. In addition, HTLV-1 proteins were detected in CD4-positive infiltrating T lymphocytes but not CNS resident cells. Although neurons were generally preserved, apoptotic oligodendrocytes were frequently in contact with CD8-positive cells; this likely resulted in demyelination. These findings suggest that the immune responses of the CTLs against HTLV-1–infected CD4-positive lymphocytes migrating into the CNS resulted in bystander neural damage.

Key Words: Apoptosis, Cytotoxic T lymphocyte, Demyelination, HTLV-1–associated myelopathy/tropical spastic paraparesis (HAM/TSP), Human T-lymphotropic virus type-1 (HTLV-1).

From the Department of Neurology and Geriatrics (EM, HT) and Center for Chronic Viral Diseases (RK, SI), Kagoshima University Graduate School of Medical and Dental Sciences, Kagoshima; and Department of Immunology, University of the Ryukyus, Okinawa (YT), Japan.

Send correspondence and reprint requests to: Ryuji Kubota, MD, PhD, Center for Chronic Viral Diseases, Kagoshima University Graduate School of Medical and Dental Sciences, 8-35-1 Sakuragaoka, Kagoshima 890-8544, Japan; E-mail: kubotar@m2.kufm.kagoshima-u.ac.jp

This work was supported by Health and Labour Sciences Research Grants from the Ministry of Health, Labour and Welfare of Japan and JSPS KAKENHI Grants 25293205 and 24133701 from the Ministry of Education, Culture, Sports, Science, and Technology of Japan.

The authors declare no conflict of interest.

Supplemental digital content is available for this article. Direct URL citations appear in the printed text and are provided in the HTML and PDF versions of this article on the journal's Web site (www.jneuropath.com).

INTRODUCTION

Human T-lymphotropic virus type 1 (HTLV-1) infection is estimated to affect 1 to 2 × 10^7 people worldwide. Although HTLV-1 infection is lifelong, the majority of infected individuals remain asymptomatic; only 1% to 2% of these individuals develop HTLV-1–associated diseases, including adult T-cell leukemia/lymphoma (1), and a range of chronic inflammatory diseases, including myelopathy (2–4), uveitis (5), arthritis (6), polymyositis (7, 8), inclusion-body myositis (9, 10), and alveolitis (11). The most recognized inflammatory disease is HTLV-1–associated myelopathy/tropical spastic paraparesis (HAM/TSP), in which CNS lesions correspond to progressive weakness of the lower extremities, with spasticity, urinary incontinence, and mild sensory disturbance. Patients with HAM/TSP exhibit higher HTLV-1 proviral load in the peripheral blood mononuclear cells (PBMCs) than asymptomatic HTLV-1 carriers (12). Furthermore, HTLV-1–infected cells accumulate in the cerebrospinal fluid (CSF) on neurologic exacerbation (13). One of the most striking features of the cellular immune response in patients with HAM/TSP is the highly elevated numbers of HTLV-1–specific CD8-positive cytotoxic T lymphocytes (CTLs) in PBMCs compared with asymptomatic HTLV-1 carriers (14, 15). These CTLs produce proinflammatory cytokines (16, 17). The HTLV-1–specific CTLs are thought to be a key factor in the pathogenesis of HAM/TSP (18, 19). This persistently activated CTL immune response to HTLV-1 provides unequivocal evidence of persistent HTLV-1 antigen expression in vivo. To date, no previous studies have shown CTLs and HTLV-1 proteins in CNS tissues from patients with HAM/TSP.

Although Skinner et al visualized antigen-specific T cells with nonfrozen tissues (20), the method has not been adapted to frozen tissue samples. In this study, we established novel in situ staining methods for detecting virus-specific CTLs and HTLV-1 proteins in frozen human tissue samples. We detected a number of HTLV-1–specific CTLs and HTLV-1–infected CD4-positive cells infiltrating the CNS and verified the bystander hypothesis that the interaction between HTLV-1–specific CTLs and HTLV-1–infected T lymphocytes causes damage to bystander neural cells in the CNS (21).

MATERIALS AND METHODS

Subjects

We obtained autopsied spinal cord tissue from 9 HAM/TSP patients after obtaining written informed consent from their

TABLE 1. Patient Clinical Data

Patient ID	Age, years/Sex	Duration of Illness, years	Cause of Death	Cellular Infiltration[a]	Human T-Lymphotropic Virus Type-1 Antibody Titer[b]	HLA[c]
8624	59/Male	7	Pulmonary tuberculosis	3+	512×	A*02 + A*24-
6315	71/Female	4.5	Bacterial pneumonia	3+	32,768×	A*02-A*24+
6664	52/Female	8	Pontine hemorrhage	1+	131,072×	A*02 + A*24+

[a] Cellular infiltration: a degree of cellular infiltration in the spinal cord.
[b] The antibody titer in serum was determined by particle agglutination method.
[c] HLA: human leukocyte antigen.

family members and stored them at −80°C until use. Human T-lymphotropic virus type 1 Tax11-19 (LLFGYPVYV) and Tax301-309 (SFHSLHLLF) are well-characterized immunodominant epitopes that are restricted to HLA-A*02 and HLA-A*24, respectively (22, 23). Human leukocyte antigen (HLA) typing was performed in all of the autopsied samples (24). Three samples were found suitable for use in this study. The first was from an HLA-A*02–positive patient (No. 8624), the second was from an HLA-A*24–positive patient (No. 6315), and the third was from an HLA-A*02 and HLA-A*24 double–positive patient (No. 6664). We had frozen block samples from entire levels of the spinal cord of each patient. We first evaluated each block by routine histology and used the samples with inflammatory lesions for the study. The clinical characteristics of the patients are shown in Table 1. This study was approved by the Kagoshima University Ethics Committee.

Immunohistochemistry

Primary and secondary antibodies are listed in Table 2. Fresh-frozen spinal cord samples were cut into 8-μm-thick sections, placed on aminosilane-coated slides, and dried for 3 hours. After fixation with 4% paraformaldehyde (PFA) in PBS for 20 minutes at room temperature (RT), the sections were incubated with a primary monoclonal antibody (mAb) for 60 minutes at RT. The samples were washed with PBS after each step.

For immunohistochemistry, the sections were treated with 3% H_2O_2 in PBS for 20 minutes and subsequently incubated with horseradish peroxidase–labeled polymer-conjugated anti-mouse antibody (Ab) reagent (EnVision+ reagent; Dako, Tokyo, Japan) for 30 minutes at RT. Finally, peroxidase was visualized using 3-amino-9-ethylcarbazole (AEC) substrate as the red color. The sections were counterstained with hematoxylin and analyzed by light microscopy.

For immunofluorescence staining, the sections were incubated with fluorescence-conjugated secondary antibodies for 60 minutes at RT in the dark. The sections were counterstained with 4′,6-diamidino-2-phenylindole (DAPI) and analyzed using a confocal laser scanning microscope (FV500; Olympus, Tokyo, Japan). For double staining, 2 primary antibodies with

TABLE 2. Primary and Secondary Antibodies Used for Immunohistochemical Studies

Antibody	Dilution	Company
Mouse anti-CD4 mAb (4B12, IgG1)	50×	Dako, Tokyo, Japan
Rat anti-CD4 mAb (YNB46.1.8, IgG)	50×	Abcam, Tokyo, Japan
Mouse anti-CD3 mAb (UCHT1, IgG1)	50×	Beckman Coulter, Tokyo, Japan
Mouse anti-CD8 mAb (DK25, IgG1)	50×	Dako
Mouse anti-CD68 mAb (KP-1, IgG1)	400×	Dako
Mouse anti–HTLV-1 Tax mAb (Lt-4, IgG3)	250×	Not applicable*
Mouse anti–HTLV-1 Gag mAb (TP-7, IgG1)	400×	Abcam
Mouse anti–HTLV-1 Env mAb (65/6C2, IgG1)	2000×	Abcam
Rabbit anti–Ki-67 Ab (IgG)	100×	Abcam
Mouse anti–granzyme B mAb (GB11, IgG1)	50×	Serotec, Kidlington, UK
Mouse anti–IFN-γ mAb (45.15, IgG1)	500×	Ancell, Bayport, MN
Mouse anti-CNPase mAb (11-5B, IgG1)	400×	Millipore, Tokyo, Japan
Mouse anti-GFAP mAb (6 F2, IgG1)	250×	Dako
Mouse anti-perforin mAb (δG9, IgG2b)	200×	BioVision, Milpitas, CA
Rabbit anti-PE Ab	500×	BioGenesis, Westminster, CO
Rabbit anti–active caspase-3 mAb (E83-77, IgG)	50×	Epitomics, Burlingame, CA
Rabbit anti–single-stranded DNA (ss DNA) Ab (F7-26)	50×	Abcam
Alexa Fluor 488-, 594- or 647–conjugated goat anti-mouse IgG1 or IgG3 Abs	1000×	Invitrogen, Tokyo, Japan
Alexa Fluor 488–conjugated goat anti-rabbit IgG Ab	1000×	Invitrogen
Alexa Fluor 488–conjugated goat anti-rat IgG Ab	1000×	Invitrogen

*Described in Lee et al (25).
Ab, antibody; CNPase, 2′,3′-cyclic-nucleotide 3′-phosphodiesterase; GFAP, glial fibrillary acidic protein; HTLV-1, human T-lymphotrophic virus-1; IFN-γ, interferon-γ; mAb, monoclonal antibody.

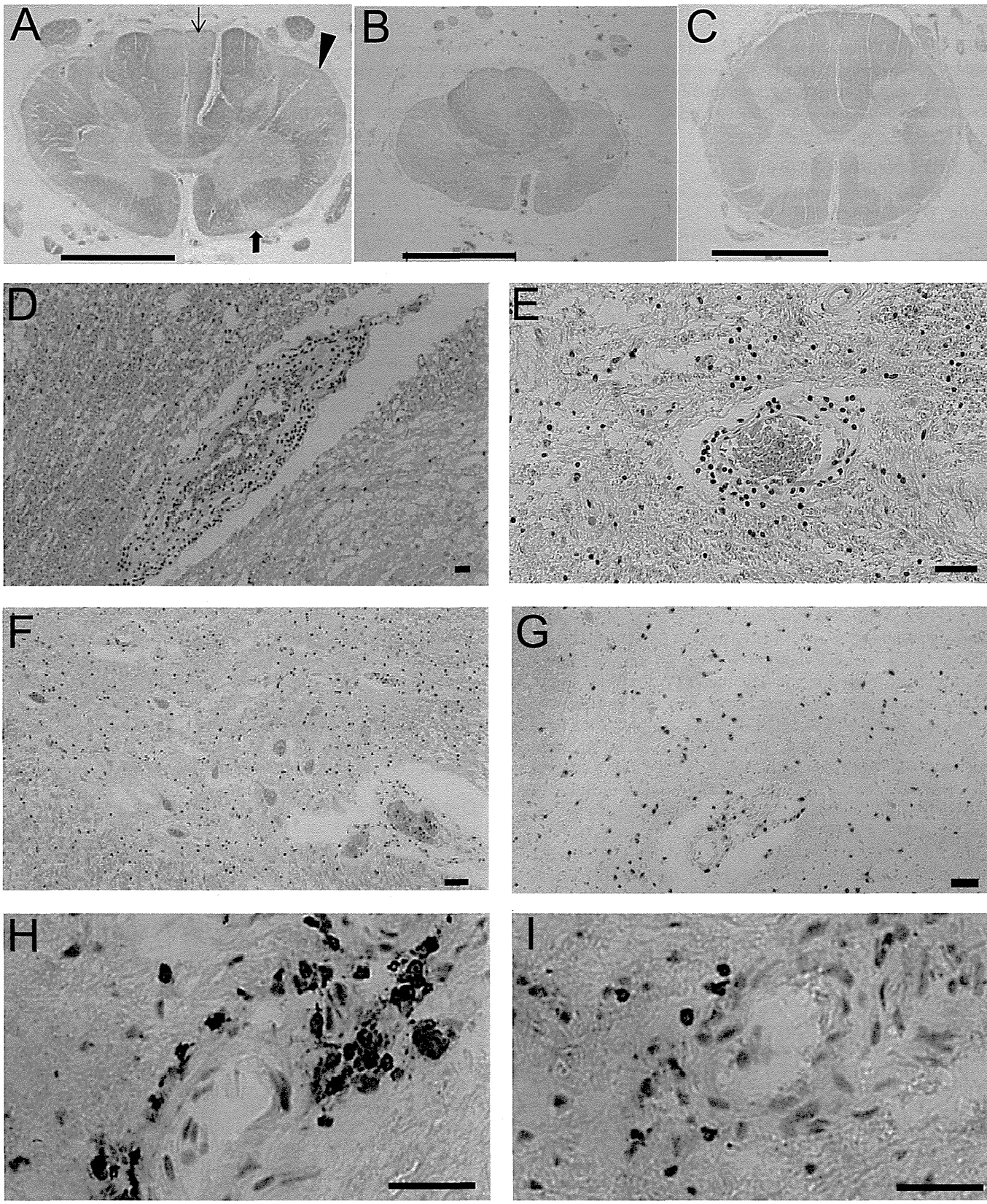

different immunoglobulin subclasses reacted to the sections simultaneously overnight at 4°C. The sections were incubated with 2 Alexa Fluor–conjugated secondary antibodies for relevant immunoglobulin subclasses. For multicolor staining, we always obtained images by sequentially scanning with each laser line to avoid the fluorescence bleeding. The sections were evaluated by 2 investigators.

In Situ Tetramer Staining

HTLV-1 Tax–specific T lymphocytes were detected with either phycoerythrin (PE)-labeled HLA-A*0201/Tax11-19-tetramer or HLA-A*2402/Tax301-309-tetramer (MBL, Japan) diluted to 1.0 μg/mL. HLA-A*0201/Tax11-19-pentamer was also used to corroborate the results of the tetramer in the staining of the CNS. Phycoerythrin-labeled HLA-A*0201/HIV Gag peptide (SLYNTVATL) tetramer or PE-labeled HLA-A*2402/HIV Env peptide (RYLKDQQLL) tetramer was used as an irrelevant control. The sections were fixed with PBS-buffered 0.1% PFA for 10 minutes and washed with PBS after each step. The sections were incubated with tetramer overnight at 4°C in the presence of proteinase inhibitors (Roche, Tokyo, Japan) and subsequently fixed again with PBS-buffered 4% PFA for 20 minutes at RT. Rabbit anti-PE Ab (500×; BioGenesis, Westminister, CO) was used as the secondary Ab and incubated with the sections for 60 minutes at RT. The signal was enhanced with the EnVision+ system and visualized with AEC chromogen. For immunofluorescence staining, the sections were incubated with goat anti-rabbit Ab labeled with Alexa Fluor 488 for 60 minutes at RT. For double staining, sections were simultaneously incubated with any of anti-CD8 mAb, anti–granzyme B mAb, anti–interferon-γ (IFN-γ) mAb, or Lt-4 mAb and with Tax-tetramer. After overnight incubation and fixation, the sections were incubated with rabbit anti-PE Ab for 60 minutes. The sections were then incubated with Alexa Fluor 594–conjugated anti–mouse IgG1 or IgG3 Ab and Alexa Fluor 488–conjugated goat anti-rabbit IgG Ab for 60 minutes at RT. 4′,6-Diamidino-2-phenylindole was used for counterstaining. To determine the frequency of Tax-tetramer–positive cells among the CD8-positive cells, we counted the cells under full-field observation (400×).

Detection of HTLV-1–Infected Cells in the Tissues

Fresh-frozen spinal cord sections were used to detect HTLV-1 proteins. The sections were dried and fixed with 4% PFA for 20 minutes at RT. Anti–HTLV-1 Tax mAb (Lt-4), anti–HTLV-1 Gag mAb (TP-7), or anti–HTLV-1 Env mAb (65/6C2) was applied to the sections in combination with anti-CD3 mAb, anti-CD4 mAb, or anti–Ki-67 Ab. After the sections were incubated overnight at 4°C, they were incubated with isotype-specific secondary antibodies for 60 minutes at RT in the dark and subsequently counterstained with DAPI.

Detection of Apoptotic Cells

Apoptotic cells were detected with anti–active caspase-3 Ab or anti–single-stranded DNA Ab by light microscopy and confocal laser scanning microscopy. The cells were also detected with TdT-mediated dUTP nick end labeling method according to the manufacturer's instructions (ApopTag Millipore, Billerica, MA).

RESULTS

General Findings in the CNS of HAM/TSP Patients

Transverse sections of the spinal cords of HAM/TSP patients demonstrated atrophy in the lateral columns with thickened meninges (Fig. 1A–C). Symmetric patchy myelin pallor in Luxol fast blue staining was observed in the affected long tracts, lateral cerebrospinal fasciculus, ventral and dorsal spinocerebellar fasciculi, spinothalamic fasciculus in the lateral column, and fasciculus gracilis in the posterior columns. The essential histopathologic feature was a chronic progressive inflammatory process with marked parenchymal exudation of lymphocytes and macrophages around the vessels (i.e. postcapillary venules) in both the gray and white matter of the spinal cord (Fig. 1D, E). The degree of cellular infiltration was strong in Patients 6315 and 8624, whereas Patient 6664 had no significant cell infiltrates (Table 1). Neurons in the anterior horns were generally preserved (Fig. 1F). Immunohistochemical staining of the spinal cord revealed remarkable infiltration of CD8-positive cells (Fig. 1G, H) and CD4-positive cells (Fig. 1I) and macrophages (data not shown) throughout the parenchyma, especially in perivascular areas. These histochemical findings are consistent with previous reports.

Detection of HTLV-1 Tax–Specific CTLs in the CNS

To validate the in situ tetramer staining procedure for visualization of HTLV-1–specific CTLs, PBMCs of HLA-A*02–positive patients with HAM/TSP were fixed on slides and stained with HLA-A*02/Tax11-19 tetramer and anti-CD8 mAb. The fluorescence pattern of the tetramer exactly colocalized with that of anti-CD8 mAb on the PBMCs (Fig. 2A). This is consistent with the fact that CD8 cells express a T-cell

FIGURE 1. Routine and histochemical study of spinal cords from patients with HTLV-1–associated myelopathy/tropical spastic paraparesis (HAM/TSP) by light microscopy. **(A–C)** The spinal cord (**A**, cervical level; **B**, lower thoracic level; **C**, lumbar level) of a HAM/TSP patient shows marked atrophy in the lateral columns; original magnification is 40×. The bars indicate 3 mm. **(A)** Symmetric myelin pallor is noted in the lateral cerebrospinal fasciculus, ventral and dorsal spinocerebellar fasciculus, lateral spinothalamic fasciculus in the lateral column (arrowhead), anterior spinothalamic fasciculus in the anterior column (thick arrow), and fasciculus gracilis in the posterior column (thin arrow). **(B)** There is marked atrophy, particularly of the lateral column. **(C)** Mild atrophy in the lumbar level. **(D)** A number of infiltrating cells are scattered throughout the section of the spinal cord. **(E)** Perivascular and parenchymal mononuclear cell infiltrates. **(F)** Neurons in the anterior horn are fairly preserved in the atrophied spinal cord. **(G, H)** Immunohistochemical study revealed that markedly infiltrating CD8-positive cells (red) are scattered in the parenchyma and around a small vessel in the spinal cord. **(I)** CD4-positive cells (red) are observed around a small vessel in the spinal cord. Nuclei were counterstained with hematoxylin (**D–I**, blue). Scale bar = 100 μm. **(A–C)** Luxol fast blue; **(D–F)** hematoxylin and eosin; **(G–I)** immunohistochemistry with hematoxylin counterstain.

receptor. We could not detect HTLV-1–specific CTLs at all with Tax-tetramer or -pentamer in frozen samples using a reported procedure for nonfrozen samples (20). We tested several modified staining procedures and finally found that prefixing the frozen sections at a very low concentration of PFA was optimal. We selected the sections that stained best with the tetramer or pentamer from several sections from each block. We detected HTLV-1 Tax11-19–specific CTLs in the parenchyma of the spinal cords from an HLA-A*02–positive patient (Fig. 2B) and an HLA-A*24–positive patient (Fig. 2C) with HLA-A*02/Tax-tetramer and HLA-A*24/Tax-tetramer, respectively. The CTLs were also detected in the thickened leptomeninges (Fig. 2D). On the other hand, no cells were detected by HIV Gag-tetramer and influenza-tetramer as tetramer controls (Fig. 2E).

Accumulation of HTLV-1 Tax–Specific CD8-positive CTLs in the CNS

To determine the frequency of HTLV-1 Tax–specific CTLs in CD8-positive lymphocytes infiltrating the CNS, we performed double staining for HTLV-1 Tax–specific CTLs and CD8-positive lymphocytes. Tax-specific CTLs stained with Tax-tetramer were frequently noted in the lesions. Double staining revealed that the fluorescence of Tax-tetramer colocalized with that of anti-CD8 mAb in all 3 patients (Fig. 3A–C). Meanwhile, HIV-tetramer restricted by either HLA-A*02 or HLA-A*24 did not bind any CD8-positive cells in the corresponding specimen (Fig. 3D). Next, we evaluated the frequency of Tax-specific CTLs in CD8-positive lymphocytes in 4 sections of the spinal cord from each patient. The percentages of Tax-specific CTLs in CD8-positive cells were 22.1% (62 of 280) and 31.1% (96 of 309) in patients with HLA-A*02–positive and HLA-A*24–positive patients, respectively (Table 3). Patient 6664 had no significant cellular infiltrates, and we only detected 2 HLA-A*24/Tax-tetramer–positive and no HLA-A*02/Tax-tetramer–positive cells in the 4 sections of the spinal cord from that patient. In addition to Tax-tetramer, Tax-pentamer was also used for the staining of the tissues from Patient 8624 to corroborate our results with Tax-tetramer. Similarly, the fluorescence of Tax-pentamer exactly colocalized with that of anti-CD8 mAb; the frequency of Tax-pentamer–positive cells in CD8-positive cells was 31% in the lesion (Fig. 3E).

Detection of HTLV-1 Proteins in the CNS

Although the HTLV-1 gene has been detected in CD4-positive lymphocytes, its viral protein has not been detected in freshly isolated lymphocytes. Therefore, we used HTLV-1–infected cell lines in a preliminary study for visualizing HTLV-1 Tax protein. Detected HTLV-1 Tax showed a patchy staining pattern in the nuclei of a human cell line (Figure, Supplemental Digital Content 1, parts A and B, http://links.lww.com/NEN/A676). Although HTLV-1 Tax was not detected in noncultured PBMCs, we detected the protein in PBMCs of patients with HAM/TSP after 8-hour culture (Figure, Supplemental Digital Content 1, part C, http://links.lww.com/NEN/A676).

We next detected 3 HTLV-1 proteins (Tax, Env, and Gag) in the CNS tissues of the HAM-TSP patients. Tax was found in the cells near vessels (Fig. 4A, B) and in the leptomeninges. The nuclear protein Tax showed a patchy staining pattern in the nuclei (Fig. 4C, D, G), whereas Env and Gag were detected in the cell membrane or cytoplasm (Fig. 4E–G). Double staining revealed that the cells expressing Tax, Env, or Gag were CD4-positive lymphocytes (Fig. 4C–F). CD68-, CD8-, CNPase-, and glial fibrillary acidic protein (GFAP)–positive cells were not positive for HTLV-1 Tax (Figure, Supplemental Digital Content 2, http://links.lww.com/NEN/A677). To investigate whether HTLV-1–infected cells proliferate in the CNS, we stained with anti-Tax mAb and anti–Ki-67 Ab (a marker of cell proliferation); however, Ki-67–positive Tax-positive cells were very rare; we detected only 2 cells in the 2 sections (data not shown). To investigate the frequency of HTLV-1–infected cells in the CD4-positive population and the frequency of apoptotic cells in HTLV-1–infected cells, we performed triple staining for CD4, active caspase-3, and HTLV-1 Env protein. The HTLV-1–positive cells in infiltrating CD4-positive cells were 60.3% and 82.4% in Patients 8624 and 6315, respectively (Table 3). More than 50% of infiltrating CD4-positive cells were infected with HTLV-1. Furthermore, HTLV-1–infected cells had a greater tendency to undergo apoptosis than noninfected cells; 36.4% of the infected cells were undergoing apoptosis, whereas 10.3% of noninfected cells were undergoing apoptosis in Patient 8624 (Table 3). Because the sample from Patient 6664 showed only a few cellular infiltrates, we could not evaluate the frequency of apoptosis in that case.

Functional Molecules of HTLV-1–Specific CD8-Positive CTLs

To investigate whether HTLV-1 Tax–specific CD8-positive CTLs have the ability to attack HTLV-1–infected CD4-positive cells in the CNS, we attempted to detect functional molecules of CTLs in the CNS. Granzyme B–, perforin-, and IFN-γ–positive cells were detected in both parenchymal and perivascular areas (Fig. 5A–C). Some of the cells stained with Tax-tetramer were positive for granzyme B (Fig. 5D). Furthermore, double staining revealed that CD8-positive cells sometimes were in contact with HTLV-1–infected cells (Fig. 5E), and that some HTLV-1 Tax–specific CTLs were next to HTLV-1–infected cells in the parenchyma (Fig. 5F). Human T-lymphotropic virus type-1 Tax–specific CTLs were not positive for Ki-67 (data not shown).

Apoptotic Cells

Next, we determined which cells underwent apoptosis in the CNS of the patients. Active caspase-3–positive cells (apoptotic cells) were frequently observed near CD8-positive cells in the parenchyma of the spinal cord, and some of them were in contact with CD8-positive cells (Fig. 5G–I). Active caspase-3 showed granular staining patterns in our pictures, although it has shown a diffuse cytoplasmic pattern in previous studies. The staining pattern may differ because of the different conditions of the frozen samples. We tried to detect the apoptotic cells with formalin-fixed paraffin-embedded samples by light microscopy. Caspase-3 was detected in the cell cytoplasm in those samples (Fig. 6A). Next, we stained the sections by methods other than the anti–active caspase-3 Ab to corroborate

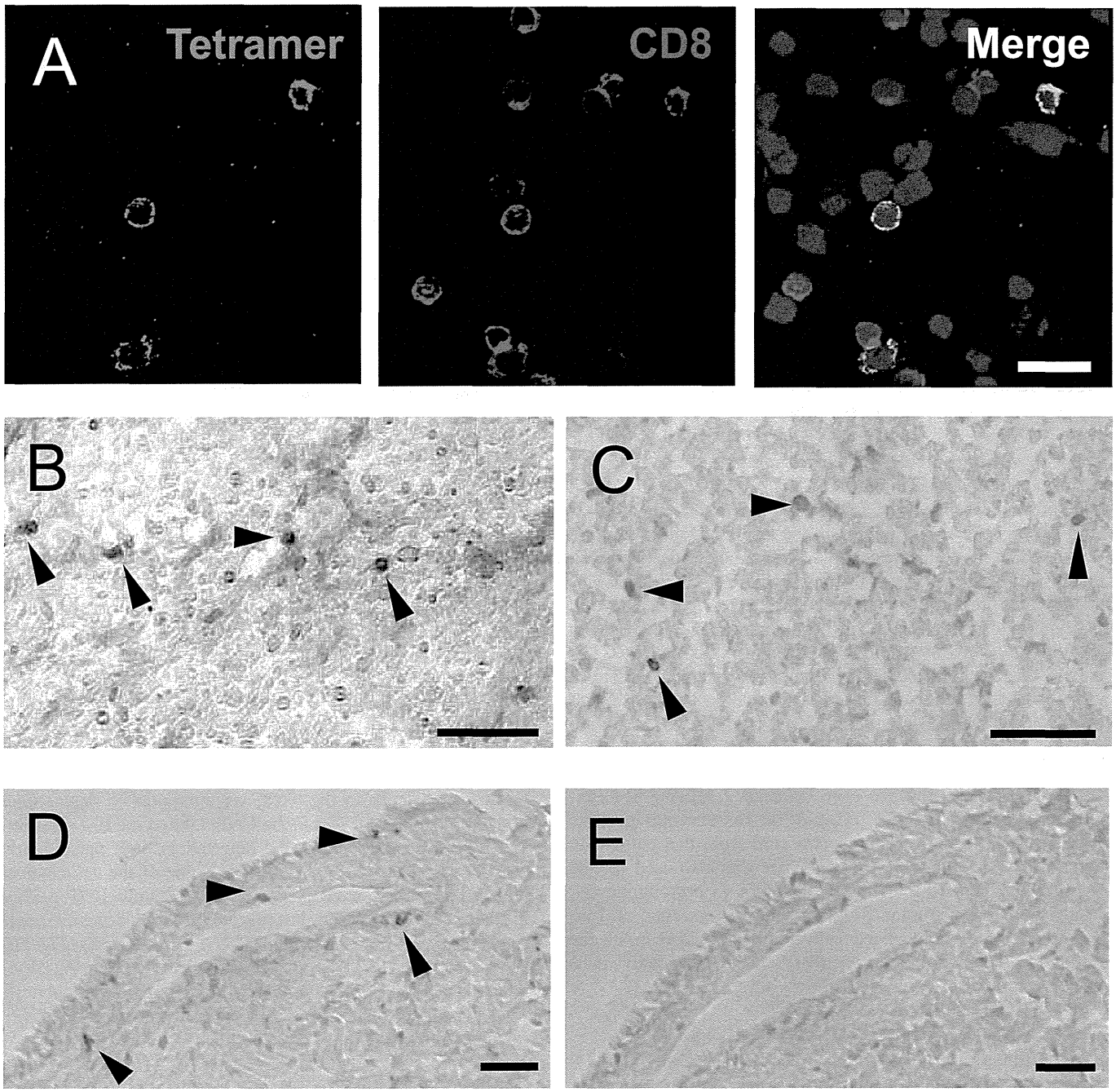

FIGURE 2. Detection of CD8-positive human T-lymphotropic virus type-1 (HTLV-1) Tax–specific cytotoxic T lymphocytes (CTLs) in peripheral blood mononuclear cells (PBMCs) and CNS. **(A)** Double staining with anti-CD8 monoclonal antibody (red) and HLA-A*0201/Tax11-19 or HLA-A*2402/Tax11-19 tetramer (green) was performed with confocal laser scanning microscopy (CLSM). DAPI (blue) was used for counterstaining the nuclei. The 3 colors were captured sequentially using CLSM. Merged images are shown on the right. PBMCs from a patient with HAM/TSP are stained with the tetramer. **(B)** HLA-A*0201/Tax11-19-tetramer–positive cells are scattered in the spinal cord parenchyma (Patient 8624). **(C)** HLA-A*2402/Tax301-309-tetramer–positive cells are seen in the parenchyma of the spinal cord (Patient 6315). **(D)** Cells stained with HLA-A*0201/Tax11-19-tetramer are found around the vessel in the spinal cord leptomeninges (Patient 8624) (red). **(E)** No cells are stained with HLA-A*0201/HIV Gag-tetramer in the adjacent serial section. White and black bars indicate 20 μm and 100 μm, respectively.

the frequent apoptosis in the spinal cord. Using a TdT-mediated dUTP nick end labeling assay, we detected a number of apoptotic cells (Fig. 6B, C). We also stained these spinal cord samples with anti–single-stranded DNA Ab and obtained similar findings (Fig. 6E). Altogether, the 3 staining methods showed frequent apoptosis in the affected spinal cords (Fig. 6).

Double staining revealed that apoptotic cells were CD4-positive or CD68-positive cells (Fig. 7D, E). Interestingly,

oligodendrocytes, which were stained with anti-CNPase mAb (Fig. 7B), were frequently undergoing apoptosis (Fig. 7F). This finding is consistent with the occurrence of demyelination in the spinal cords of HAM/TSP patients. However, oligodendrocytes were not stained with anti–HTLV-1 Tax mAb (data not shown) or anti–HLA-ABC Ab (Fig. 7G). Astrocytes that were stained with anti-GFAP mAb were diffusely distributed throughout the parenchyma (Fig. 7A), whereas GFAP-positive cells